COMMENTARIES AND REVIEWS

This section of Journal of Materials Research is reserved for papers that are comments on topics of current interest or reviews of literature in a given area.

A review of catalytically grown carbon nanofibers

N. M. Rodriguez

Materials Research Laboratory, The Pennsylvania State University, University Park, Pennsylvania 16802

(Received 27 January 1993; accepted 2 August 1993)

Carbon nanofibers (sometimes known as carbon filaments) can be produced in a relative large scale by the catalytic decomposition of certain hydrocarbons on small metal particles. The diameter of the nanofibers is governed by that of the catalyst particles responsible for their growth. By careful manipulation of various parameters it is possible to generate carbon nanofibers in assorted conformations and at the same time also control the degree of their crystalline order. This paper is a review of the recent advances made in the development of these nanostructures, with emphasis both on the fundamental aspects surrounding the growth of the material and a discussion of the key factors which enable one to control their chemical and physical properties. Attention is also given to some of the possible applications of the nanostructures which center around the unique blend of properties exhibited by the material.

I. INTRODUCTION

The discovery of buckminsterfullerene, C_{60}, coupled with recent findings that such molecules can be arranged in the form of tubular structures[1] has generated intense research activity with the anticipation that these materials can have some unique properties and applications. The purpose of this review is to acquaint the reader with the advantages of the use of catalysts to grow analogous nanostructures and to highlight the flexibility that such a process offers for tailoring the chemical and physical properties of the material for a particular application. Carbon nanofibers (also known as carbon filaments) can be grown from the catalytic decomposition of certain hydrocarbons over small metal particles such as iron, cobalt, nickel, and some of their alloys.[2–5] The diameter of the nanostructure is controlled by the size of the catalyst particle and can vary between 2 and 100 nm, and lengths ranging from 5 to 100 μm.[3] The formation of this type of material from the interaction of carbon containing gases with hot metal surfaces was first reported in 1890[6]; however, structural details as well as mechanistic features have been the result of recent advances in electron microscopy techniques.

Diverse interests have motivated workers over the past few years to try to learn more about the mechanism of nanofiber growth as well as the measurement of the properties of the material. The prevention of carbon deposit accumulation is a high priority objective in many processes involving hydrocarbon conversion reactions, where the presence of such nanostructures creates problems including blockage of reactors, reduction of heat transfer properties, and deactivation of catalyst systems due to encapsulation of the metallic component.[7–11] On the other hand, because of the newly discovered properties of these catalytically grown carbon nanofibers, efforts are now being directed at optimizing the growth of this type of material.

The mechanism of carbon nanofiber formation has been the subject of some controversy particularly with regard to the active state of the catalyst particle responsible for the growth. The early model was developed as the result of the direct observation of the growth of individual structures by Baker and coworkers using controlled atmosphere electron microscopy.[12] In their proposed mechanism, the key steps are the adsorption and decomposition of a hydrocarbon on a metal surface to produce carbon species which dissolve and diffuse through the bulk and ultimately precipitate at the rear of the particle to form the nanofiber. As a result of this process the catalyst particle is detached from its original support and remains at the growing end of the carbon structure.

In addition to the whisker-like structure which was the basis for the proposed mechanism, several other more intricate conformations have been found including bi-directional, helical, branched, and coiled.[13–17] The detailed structure of this form of carbon has been investigated by high resolution electron microscopy[18–21] and it has been reported that the carbon nanostructures consist of a cylindrical arrangement in which the central part is less dense (more electron transparent) with a short-range crystalline order. In contrast, the outer region of the tube shows an extremely ordered arrangement in which individual graphite platelets are usually aligned parallel to the side faces of the catalyst particle.

Audier and coworkers[22] studied the effect of temperature and catalyst composition on the morphology

of carbon deposits produced by the decomposition of CO and CH_4 over a number of catalysts. They found that extremely marked physical differences could be encountered in the nanofibers that were entirely dependent on the chemical nature of the catalyst. Tubes (hollow cored structures), bi-tubes (with the catalyst particle enclosed), solid structures, and shells were observed. Careful examination indicated that these morphologies were determined by the physical conformation adopted by the catalyst. The tubular conformation was explained in terms of a model put forward by Tibbetts[23] in which he proposed that graphite planes would adopt a cylindrical strained structure where the diameter is governed by the size of the associated catalyst particle. The model predicts that there is a minimum diameter below which no fibers will grow. The smallest fiber diameter observed by transmission electron microscopy was found to be 3.5 nm for inner radius, close to that determined from theoretical calculations. According to Boellaard and coworkers,[20] who proposed another model to account for these hollow structures, the graphite planes were not aligned parallel to the axis of the filament but instead at an angle with respect to the catalyst particle, adopting a particular crystallographic orientation. Using electron diffraction analysis, they reached the conclusion that graphite precipitated from the catalyst particle with the planes parallel to the catalyst surface. It was therefore assumed that there was a face at the center of the particle that did not generate carbon deposits. In more recent studies Yang and Chen[24] used a combination of electron diffraction analysis and molecular orbital calculations and the data were interpreted according to the notion that nanofibers contained single crystal particles, where $Ni_{(111)}$ and $Ni_{(311)}$ would provide better epitaxial fit with graphite planes than would either $Ni_{(100)}$ or $Ni_{(110)}$. The formation of the diverse structures could be the result of the reconstruction of the catalyst particles to acquire distinct crystallographic orientations at the metal-carbon interface. Surface science studies[25,26] have revealed that certain faces favor precipitation of carbon whereas others are incapable of performing such a process and as a result will be free of carbon leading to the formation of hollow structures. Figueiredo and coworkers[27] demonstrated that the inner portions of carbon nanofibers, which had been formed from the interaction of nickel particles with acetylene, could be removed if the hydrocarbon was replaced with hydrogen and the specimen heated to 725 °C. Careful control of this latter step was also found to result in the formation of hollow structures.

Over recent years interest in carbon nanofibers has been stimulated as a result of the discovery of vapor grown carbon fibers. This type of material was first prepared by Koyama[28,29] via the decomposition of benzene in the presence of hydrogen over various substrates, and later extended by Endo and coworkers.[30–33] This process is carried out at temperatures between 950 and 1100 °C and involves the initial creation of carbon nanofibers, which are subsequently thickened by a non-catalytic carbon deposition route.[33] The final product consists of fibers that are relatively straight, with lengths up to 30 cm, and diameters up to 10 μm. High resolution electron microscopy studies by Oberlin and coworkers[3] indicated that the process was catalyzed by the presence of small metal particles which were originally present as impurities in the substrate. It was later demonstrated by Tibbetts and coworkers[34–36] who produced the same type of fibers on stainless steel tubes, and by Benissad and coworkers[37,38] that the benzene feed could be effectively substituted by methane. In more recent years, there has been a considerable increase in the research activity in this area driven mainly by the desire to develop more efficient and economical methods to produce vapor grown carbon fibers. To this end efforts have been directed at a fundamental understanding of the manner by which various parameters, including gas composition, nature of catalyst precursor, effect of heating rate, and reaction temperature influence the growth characteristics of the carbon fibers.[39–46] In the current review it is not the author's intention to cover the details of these microsized fibers, but instead to focus on the chemical and physical parameters associated with the nanofibers which constitute the initial stage in the growth of vapor grown carbon fibers.

Because of the extraordinary combination of physical and chemical properties exhibited by carbon nanofibers, which blends two properties that rarely coexist: high surface area and high electrical conductivity, which are the result of the unique stacking and crystalline order present within the structure, there are tremendous opportunities to exploit the potential of this form of carbon in a number of areas, some of which are discussed in this paper.

II. SYNTHESIS OF CATALYTICALLY FORMED CARBON NANOFIBERS

The preparation of bulk quantities of carbon nanofibers can be accomplished using powdered metal catalysts in a conventional flow reactor system. In a typical operation, about 100 mg of the powdered catalyst is placed in a ceramic boat which is positioned in a quartz tube located in a horizontal tube furnace. The sample is initially reduced in a 10% hydrogen-helium stream at 600 °C and then quickly brought to the desired reaction temperature. Following this step, a pre-determined mixture of hydrocarbon, hydrogen, and inert gas is introduced into the system and the reaction allowed to proceed for periods of about 2 h. Using this approach one can readily obtain 20 g quantities

of carbon nanofibers from some of the more active catalytic materials.

Over the past few years we have performed a very comprehensive evaluation of the potential of a number of metals and bimetallics as catalysts for the production of carbon nanostructures. From the data obtained from these experiments it appears that copper-nickel based alloys are among the most effective catalysts for the reaction. In addition, it is clear that hydrogen plays a major role in the production of carbon nanofibers. In some cases hydrogen acts as a promoter whereas in some systems catalyzed hydrogenation of the structures can occur, resulting in a decrease in the yield of the material.[47]

It should be emphasized that in order to produce carbon nanofibers one is not restricted to using a powdered catalyst precursor; other forms such as foils, gauzes, or supported particles are equally suitable and may provide a more simple method of handling the carbon nanofibers for a subsequent application. If the desired route is to produce the carbon nanofibers on a carbon or oxide substrate surface, then there are a number of aspects to be taken into consideration: (i) the method by which the catalyst precursor is introduced onto the substrate, (ii) the chemical properties of the substrate surface, and (iii) the nature of the interaction between the catalyst particles and the substrate surface. All these factors have a direct impact on the size and location of the catalyst particles, and the morphological characteristics of the carbon nanofibers which are produced on the substrate surface when the system is subsequently heated in a hydrocarbon environment.

Since the aim is to produce a uniform coverage of carbon nanofibers on the substrate, it is essential to establish the conditions for laying down an even dispersion of the catalyst on each type of support medium. Various methods can be used to introduce the catalyst precursor onto the substrate surface based on either aqueous or nonaqueous impregnation with solutions of metal salts or evaporation of metal containing organic compounds to generate ultrafine metal particles (<10 nm diameter).[32] Through appropriate treatment steps in oxygen followed by reduction in hydrogen, discrete particles of a desired size range can be formed on the substrate. One of the key features of the catalyst preparation method is the control of the interaction between the catalyst particles and the substrate surface. In this regard, pretreatment of the substrate surface in selected gaseous environments may prove to be a critical step in controlling the nucleation of the catalyst particles and the subsequent growth characteristics of the carbon nanostructures. During the growth process the catalyst particle is carried away from its original location and remains at the tip of the nanofiber. Finally, if necessary, the metal particles present within the solid carbon can be removed by dissolution in acid media without having any deleterious effects on the nanofiber structures.

In one particular application, which will be discussed in a later section, carbon nanofibers were grown on the sides of conventional carbon fibers.[48,49] This was not a straightforward task since carbon fibers are susceptible to attack by hydrogen and oxygen, especially in the presence of metallic impurities[50]; hence, in this case the catalyst preparation conditions had to be closely controlled in order to maintain the integrity of the parent fibers. Copper-nickel was selected as the catalyst for the generation of the carbon nanofibers and was introduced onto the support by impregnation from an aqueous solution of the mixed metal nitrates. Calcination in oxygen at 300 °C resulted in the conversion of the metal salts to mixed oxides, an essential step if one is to prevent volatilization of the catalyst precursor. Following this relatively mild oxidation treatment, neither loss of carbon nor deterioration in the carbon structure was observed. Finally, the metal oxide particles were reduced to the alloy state by reaction in a 20% hydrogen-helium mixture at 350 °C. The reduction period was found to be the key parameter with regard to the degree of metal particle growth, a factor which ultimately dictated the diameter of carbon nanofibers produced during interaction of the carbon fiber supported copper-nickel particles with an ethylene-hydrogen environment.

III. BACKGROUND

A. Mechanism of catalytic formation of carbon nanofibers

The typical appearance of a catalytically grown carbon nanofiber is shown in the transmission electron micrograph, Fig. 1(a). This structure has been produced from the decomposition of an ethylene-hydrogen mixture over a copper-nickel (3 : 7) catalyst particle at 600 °C. Examination of the electron dense catalyst shows the existence of facets both at the particle-gas and particle-solid carbon interfaces. The rudiments of the early model[12] for the formation of carbon nanofibers from the metal catalyzed decomposition of selected hydrocarbons or carbon monoxide are presented in Fig. 1(b). Initially, the hydrocarbon is adsorbed and decomposed on certain faces of the metal particle. Some of the carbon species produced in the reaction dissolve in the bulk and diffuse through the metal particle from the leading face to the rear faces where carbon is deposited from solution in the form of a nanofiber. Provided that heat balances are maintained in the system, the carbon structure will continue to grow in an interrupted fashion. Growth ceases when perturbations in the chemistry of the leading face of the particle occur which can cause the buildup of a carbon overlayer and effectively prevent further hydrocarbon decomposition.

(a)

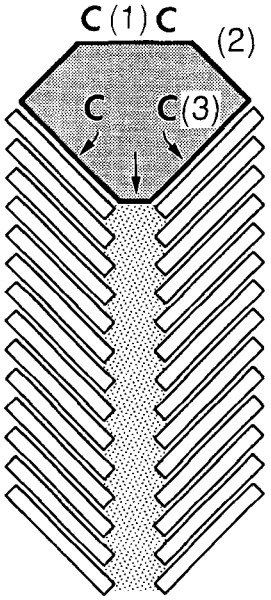

(b)

FIG. 1. (a) Transmission electron micrograph of a catalytically grown carbon nanofiber with the metal particle at the tip (reprinted with permission from Pergamon Press, Ref. 48). (b) Schematic representation showing the key steps involved in the growth of carbon nanofibers: (1) adsorption and decomposition of hydrocarbon at the metal-gas interface; (2) diffusion of dissolved carbon through catalyst particle; and (3) precipitation of carbon at the metal-nanofiber interface.

It is generally agreed that diffusion of carbon through the catalyst particle is the rate-determining step in the growth of carbon nanostructures. This is predicated on the experimental finding that the activation energies for growth of these structures exhibit a remarkable correlation with those for diffusion of carbon through the corresponding metals.[14] A comparison of the activation energies obtained from direct measurements in the controlled atmosphere electron microscope of the formation of carbon nanofibers with those values for diffusion of carbon through selected metal catalysts is presented in Table I.

The origin of the driving force for carbon diffusion through the particle is still obscure. A concentration gradient from the front face of the particle to the rear face will drive this diffusion step, and a number of studies[36,51–60] have addressed the issue of the precise nature of the thermodynamic parameters that control the process. In the first proposed mechanism,[12] it was suggested that a temperature gradient was created in the particle due to exothermic decomposition of the hydrocarbon at the front face and endothermic precipitation of solid carbon at the trailing faces. According to Sacco and coworkers,[56] a metal carbide phase was formed at the gas particle interface and the driving force for diffusion of carbon through the catalyst was established between this region and the particle-solid carbon interface. This model was later refined by Alstrup[58] who claimed that a thin carbide layer was generated on the metal surface at the particle-gas interface and that decomposition of unstable species led to supersaturation of carbon at the frontal regions of the particle, thus creating the concentration gradient required for diffusion. More recently, Lund and coworkers[59,60] have argued that it is not necessary to make the assumption that a carbide is present at the exposed regions of the particle if gas phase carbon activity is the critical parameter.

Although these proposed models provide a rational explanation for the formation of straight nanofibers and in some cases have been the basis for the development

TABLE I. Measured activation energies for carbon nanofiber growth from the metal catalyzed decomposition of acetylene.

Catalyst	Activation energy for nanotube growth[a] (kcal/mol)	Activation energy for diffusion of carbon (kcal/mol)
Nickel	34.7	33.0–34.8
α-iron	16.1	10.5–16.5
γ-iron	33.9	33.3–37.4
Nickel-iron	33.6	34.0
Cobalt	33.0–33.3	34.7
Vanadium	27.6	27.8
Molybdenum	38.8	41.0
Chromium	27.1	26.5
Ruthenium	26.2	...
Copper-nickel	31.2	...

[a]Directly measured by *in situ* electron microscopy.[5]

of procedures for inhibiting the growth of this form of carbon in commercial reactors, they all suffer from a serious shortcoming in that they fail to predict the effect of additives to the catalyst particles which bring about major perturbations in the morphological characteristics of the nanostructures.[2] Figures 2(a)–2(d) are electron micrographs showing an assortment of carbon nanofiber conformations which have been observed in systems where the catalyst was either a bimetallic or a metal which contained a small addition of certain nonmetallic elements. In addition to the whisker-like form stemming from one-dimensional growth, which was responsible for the development of the mechanism presented in Fig. 1(b), perhaps the next most common type of growth is bidirectional, Fig. 2(a). Continuous observations of the formation of this nanofiber conformation showed that growth occurred from two opposite faces of the catalyst particle, which remained located within the body of the nanofiber throughout the process. Kinetic analysis of the growth sequences obtained from controlled atmosphere electron microscopy studies demonstrated that both limbs of the structure grew at identical rates.[61] It was found that the catalyst particles associated with this growth form were always symmetrical in shape and generally adopted a diamond configuration. Audier and coworkers[62] found that such particles were polygonal with nanofibers growing around each corner and large flat facets remaining free of carbon and available for hydrocarbon adsorption and decomposition. Occasionally, in some systems the catalyst particles were observed to execute a rotary motion and this action resulted in the nanofibers acquiring a twisted form,[13] an example of which is shown in Fig. 2(b). A variation of this type of conformation is the helical structure, Fig. 2(c). Branched

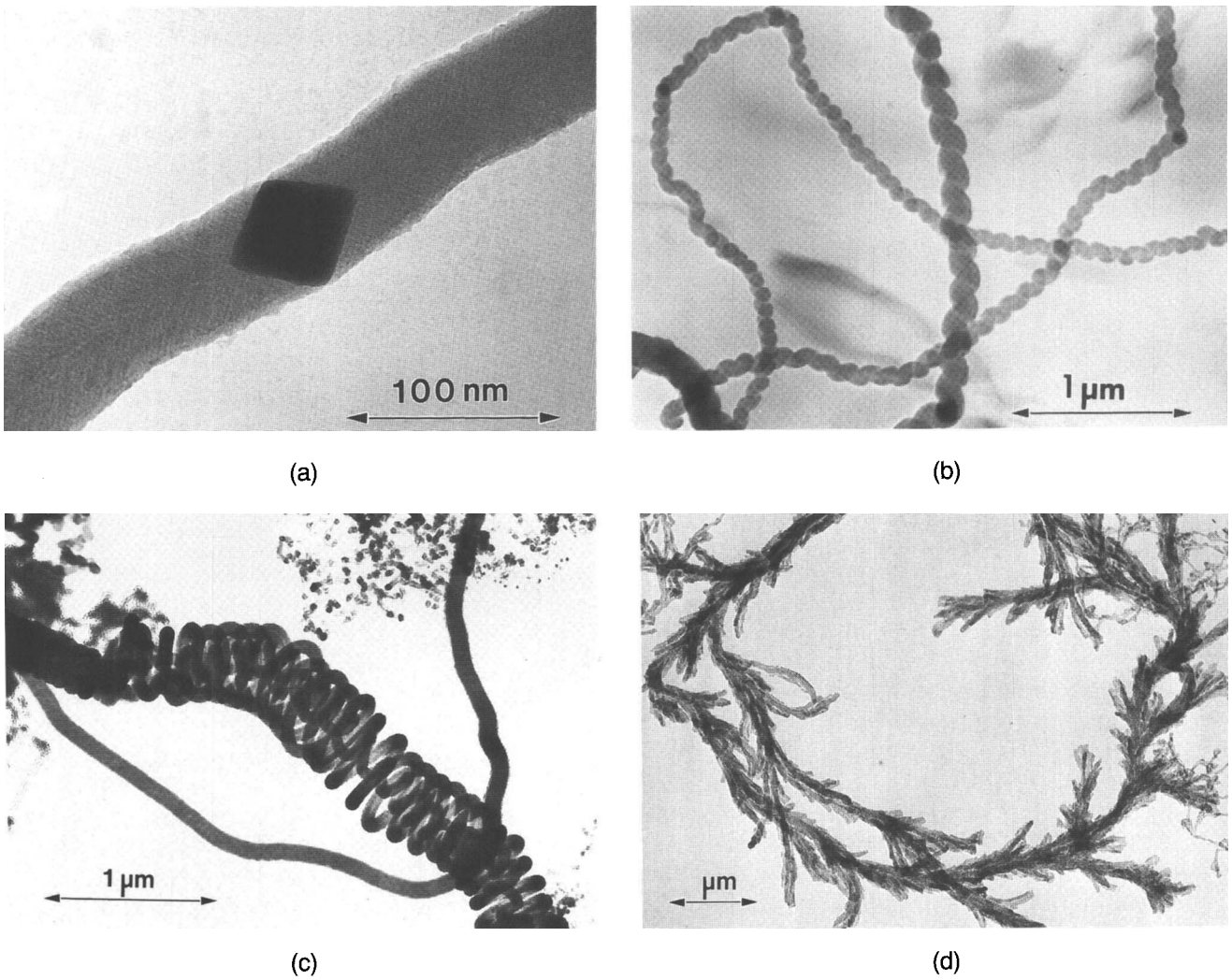

FIG. 2. Transmission electron micrographs of different types of carbon nanofibers: (a) bidirectional (reprinted with permission from Academic Press, Ref. 47); (b) twisted (reprinted with permission from Academic Press, Ref. 61); (c) helical; and (d) branched.

nanofibers, Fig. 2(d), were produced when a catalyst particle located at the growing end of a whisker-like structure suddenly "exploded" into numerous smaller particles, each of which then proceeded to generate a secondary smaller carbon nanofiber. Frequently this "explosive act" was observed just after the temperature was raised or after a given period of growth from a bimetallic catalyst where one component might have been preferentially lost from the particle due to volatilization or gradual dispersion within the solid carbon structure.[63] In this context, it is interesting to note that Benissad and coworkers[38] claimed that the catalyst particle responsible for the growth of carbon nanofibers should be in a molten state.

An examination of the catalyst particle presented in Fig. 1(a) indicates the existence of three distinct regions with respect to the carbon nanofiber formed at the rear face: (i) the catalyst/gas interface which determines the manner by which the hydrocarbon reactant molecule bonds and ultimately undergoes decomposition; (ii) the bulk of the catalyst, the chemistry of which dictates the amount of carbon dissolved and its rate of diffusion through the particle to precipitate eventually in the form of a nanofiber; and (iii) the catalyst/solid carbon interface, whose orientation is responsible for determining the structural characteristics of the material. In order to develop a comprehensive understanding of the growth and control of this form of carbon, it is essential to consider the events occurring at each of these regions.

B. Metal-gas interface

Even though carbon diffusion through the catalyst particle has been shown to be the rate-determining step,[12] a further aspect that must be taken into consideration is the manner by which the hydrocarbons bond and ultimately react with the metal surface. Prior to diffusion, a critical event must be realized in order for the process to continue, namely, the adsorption and decomposition of the reactant gas. Although many metals adsorb hydrocarbons and carbon monoxide on certain faces, this interaction does not always lead to the formation of the carbon nanostructures. In order for the process to occur, the hydrocarbon must undergo dissociative adsorption at the metal surface.

The importance of the crystallographic orientation of the metal particle in the interaction of the surface with various hydrocarbon molecules has long been recognized by surface scientists. It has been demonstrated that such features dictate not only the selectivity toward the formation of particular products, but also play a key role in determining the overall activity of the catalyst.[64,65] Furthermore, variations in the chemical nature of the gas environment can have a dramatic influence on the prevailing crystallographic characteristics of the particles. As an example, the presence of hydrogen can induce reconstruction of the exposed metal faces and cause significant changes in the catalytic action of a particular system.[66,67]

It should be appreciated that even though a series of metals may have similar surface orientations, it does not follow that they will necessarily exhibit the same characteristics with respect to the adsorption and decomposition of hydrocarbons. In this regard, it is worthwhile to compare the behavior of platinum, copper, and nickel with simple hydrocarbons. The adsorption of both ethylene and acetylene is highly favored on $Pt_{(111)}$, and it has been established that the subsequent decomposition pathways of the respective hydrocarbons is dependent on both the temperature and the degree of coverage.[68] Although the atoms in the $Cu_{(111)}$ face have identical arrangements to those in the $Pt_{(111)}$ face, the interaction of hydrocarbons with the former surface does not lead to the rupture of the carbon-carbon bonds and as a consequence a reversible chemisorption is observed.[69] In contrast, $Ni_{(111)}$ adsorbs both hydrocarbons in a dissociative manner[65] and it is expected that carbon nanostructures will be produced from such an interaction. Clearly, other factors must be taken into consideration when deciding whether adsorption of a hydrocarbon is likely to lead to decomposition. Since the development of new spectroscopic techniques including high resolution electron energy loss spectroscopy (HREELS), temperature programmed static secondary ion mass spectroscopy (TPSSIMS), and improved low energy electron diffraction techniques (LEED), it is now possible to analyze in more detail the nature of the bonding between hydrocarbon molecules and metal surfaces, e.g., C_2H_2, which was originally thought to occupy a position on top of a metal atom in $Pt_{(111)}$, is now believed[70] to adopt a distorted bridging position. Upon heating, the hydrocarbon undergoes rapid rearrangement to form an "ethylidyne" intermediate ($\equiv C-CH_3$) which is bonded to the surface by a $M\equiv C$ bond. A similar dependence is observed for the decomposition of CO on various faces of Co.[71]

While the catalytic action of pure transition metals toward the formation of carbon nanofibers during interaction with ethylene is relatively low, it has been found that their activity can be greatly enhanced by addition of an adatom, which can either be another metal (Cu, Sn, K) or a nonmetal (S).[15,40,47,72,73] Furthermore, it has been shown that gas additives such as hydrogen promote hydrocarbon decomposition with the concomitant growth of the carbon nanostructures. In this context, two possibilities exist: (i) hydrogen chemisorbed over the surface prevents condensation reactions leading to the formation of graphite overlayers,[68,74] or (ii) hydrogen adsorbed over metals weakens the metal-metal bond leading to an induced mobility of surface atoms known as faceting or

reconstruction.[75,76] The new chemisorption-induced face is less favorable toward the formation of an encapsulating overlayer, and formation of carbon nanofibers is promoted.[77] In addition to hydrogen, it has recently been shown that the introduction of controlled amounts of sulfur also enhances the catalytic conversion of hydrocarbons toward the formation of carbon nanostructures,[78] and it is also claimed that the presence of a small amount of sulfur promotes reconstruction of the metal surface.

Hydrocarbons such as ethylene and acetylene can be adsorbed on metal surfaces in two structural arrangements, "parallel" to the surface as illustrated in Fig. 3(a), or "end-on" as depicted in Fig. 3(b).[47] Configuration (a) would favor the polymerization-condensation reaction, whereas (b) would transform into "ethylidyne" and ultimately decompose to produce solid carbon and methane. Pure metals appear to adsorb ethylene preferably in conformation (a) whereas bimetallic systems and metal surfaces containing adatoms which do not themselves interact with hydrocarbons tend to promote the existence of both conformations. Usually the decomposition of the hydrocarbon in the latter case is much higher since the tendency for catalyst deactivation via the formation of a graphitic overlayer is reduced. Instead, carbon species formed at the surface can now follow an alternative pathway which involves dissolution in the metal followed by diffusion and eventual precipitation at the rear faces to form the carbon nanostructure.

C. Bulk chemical state of the catalyst

The state of the catalyst in carbon deposition has been the source of considerable controversy over the years, particularly in cases where the chemical state of the bulk of the particle could either be metallic or a metal carbide. Electron diffraction analysis of the catalyst particles after the interaction of iron with benzene/hydrogen was carried out by Oberlin and coworkers[3] and revealed the existence of cementite, Fe_3C. Postreaction examination of iron particles that had been reacted in carbon monoxide was also performed by Audier and coworkers using selected area electron diffraction techniques, and this analysis showed the presence of several carbides including Fe_5C_2 and Fe_3C.[79] Although the electron diffraction analysis did not provide evidence for the presence of metallic iron, complementary Mössbauer spectroscopic studies of the same particles indicated the coexistence of γ–Fe and metal carbides. The claim that cementite was the active phase was refuted by Baker and coworkers[80] who studied the reactivity of various iron oxides and carbides. When high purity cementite was the starting catalyst, growth of carbon nanofibers was not observed. Work performed by Yang and Yang[81] on the effect of hydrogen on carbon deposition demonstrated that the surface of Fe_3C was essentially inactive for benzene decomposition. In the presence of H_2, however, the metallic phase was generated and the activity toward carbon nanofiber growth was restored.

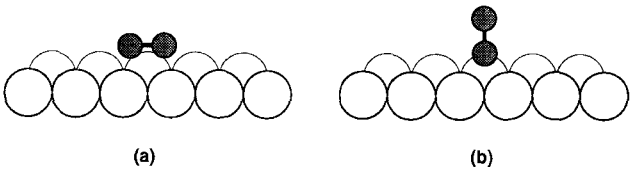

FIG. 3. Structural arrangements for (a) ethylene bonded "parallel" to the catalyst surface and (b) ethylene adsorbed in an "end-on" configuration.

The determination of the chemical state of the catalyst under reaction conditions has been the main limitation in the mechanistic studies. This restriction has been removed with the development of *in situ* electron diffraction techniques which allow one to determine the state of the particles supported on graphite in the presence of a hydrocarbon at reaction temperature.[82] Rodriguez and coworkers[83] investigated the catalyst deactivation phenomenon associated with the interaction of copper-nickel particles with ethylene at temperatures in excess of 750 °C. They reported that Cu–Ni alloys exhibited a high activity toward the production of carbon nanofibers during reaction in ethylene/hydrogen mixtures; however, as temperature was progressively raised, the catalyst lost its activity. Lowering of the temperature to a previously active regime resulted in regeneration of catalytic action, indicating that the deactivation behavior was reversible in nature. *In situ* electron diffraction analysis demonstrated that the metal catalyst was active in the region where the copper-nickel alloy was the stable phase and that the loss of activity coincided with separation into its pure components. It was significant that no evidence for the existence of a bulk carbide was found in these experiments.

If one were to accept the argument that the active catalytic phase was a bulk transition metal carbide,[56] then it would be difficult to rationalize such a claim according to the measured kinetic parameters for carbon nanofiber growth, where the values of activation energies are found to correlate with those for carbon diffusion through the respective metals, as presented in Table I.[5] Although the experimental data available contradict the role of a bulk metal carbides as being the active catalytic entity in the formation of these nanostructures, the role of a surface carbide species should not be dismissed. As discussed earlier, it is well known from surface science studies that when hydrocarbon molecules interact with metal surfaces an assortment of intermediate states can be formed, where the carbon atom in the reactant is linked to the surface by single or multiple bonds. Decomposition of these intermediates leads to the formation of the so-called carbidic carbon which proceeds to dissolve in the bulk and eventually precipitates, thus contributing to the

formation of a nanofiber. Carbidic carbon is defined as a surface metal carbide which possesses extraordinarily high activity compared to that of a bulk carbide.[25,84]

D. Metal-graphite interface

It has recently been suggested that there is a subtle relationship between the degree of ordering in the deposited carbon nanofibers and the ability of the metal catalyst particle to undergo a strong interaction with graphite in the presence of hydrogen.[61] Using post-reaction selected area electron diffraction techniques, Yang and Chen[24] found that the crystallographic orientation of the catalyst particle surface in contact with the gaseous reactant could be significantly different from that which existed at the catalyst/solid carbon interface. In addition, they showed that the nature of the deposited carbon was extremely sensitive to the orientation of the catalyst particle surface in contact with the solid carbon. Audier and coworkers used selected area electron diffraction analysis to determine the relationship between the crystallographic face of the particle and the carbon structure.[85] They reported that in the case of Fe containing alloys with a bcc structure, the catalyst particle was a single crystal, which was oriented with its [100] direction parallel to the carbon fiber axis.

The geometry of a metal particle interacting with a graphite support is governed to a large degree by the strength of the interaction between the metal atoms and the graphite support. Figure 4 is a schematic representation of the forces involved in the interaction of a metal catalyst particle with a graphite support in the presence of a gas environment. The contact angle, Θ, is determined by the surface energy of the graphite support, γGS, the surface energy of the metal, γMG, and the metal-graphite interfacial energy, γMS, and is expressed in terms of Young's equation:

$$\gamma GS = \gamma MS + \gamma MG \cos\Theta$$

Under conditions where the interactive forces between the two components are relatively weak (γMG > γGS), the contact angle is > than 90° and the particles will assume the energetically favored shape of a hemisphere [Fig. 4(a)]. In contrast, where strong forces exist between the metal and the graphite, then the contact angle will be <90° and wetting will occur [Fig. 4(b)]. In the extreme case, when the work of adhesion exceeds the work of cohesion within the particle (γMS > γGS + γMG), the metal will spread in the form of a thin film over the graphite support surface [Fig. 4(c)].[86,87] Controlled atmosphere electron microscopy studies[50] have enabled one to conclude that metals which readily undergo such a spreading action along graphite edge regions under reducing conditions also tend to produce highly graphitic carbon nanostructures when these metals are reacted in a hydrocarbon environment. Based on this relationship it is now possible to control the chemical nature of the carbon structures and predict the likely type of nanofiber that would be produced from the decomposition of a hydrocarbon over a particular metal catalyst. The data presented in Table II show the respective temperatures at which various metals and alloys exhibit a strong spreading interaction with graphite, and these values are correlated with either the observed or predicted nature of nanofiber that are formed from the metal catalyzed decomposition of ethylene/hydrogen mixtures between 500 and 600 °C.

It is apparent that cobalt, which readily undergoes a spreading action with graphite at 400 °C, forms highly graphitic carbon nanostructures, whereas other metals in the same group, iron and nickel, exhibit a somewhat

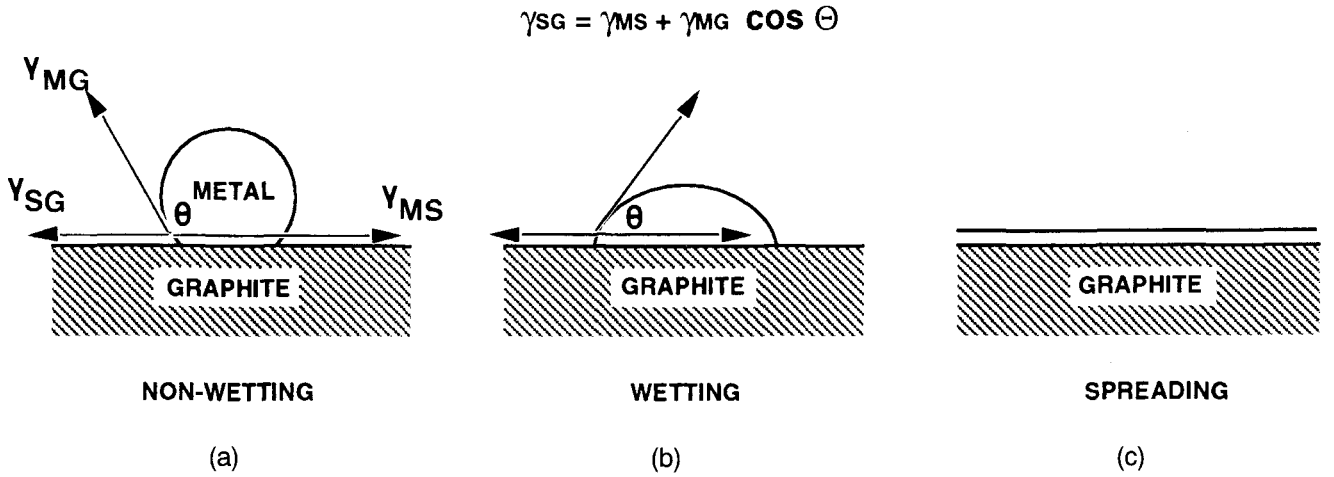

FIG. 4. Changes in metal particle shape as a function of the degree of wetting of the catalyst on graphite (Ref. 50 with permission). (a) When weak forces occur between the metal and graphite and the contact angle is >90°, no wetting occurs. (b) When strong forces occur between the two components, the contact angle is <90° and wetting occurs. In (c), when adhesion exceeds cohesion within the particle ($\gamma_{MS} > \gamma_{GS} + \gamma_{MG}$), the metal spreads over the graphite support surface.

TABLE II. Correlation between wetting properties of metals on graphite in hydrogen and crystallinity of carbon nanofibers at 600 °C.

Metal	Spreading temperature[a] (°C)	Type of carbon nanostructure[b]
Iron	>1000	Amorphous
Nickel	975	Amorphous
Cobalt	400	Highly graphitic
Platinum	755	Partially graphitic
Copper-nickel (3 : 7)	675	Moderately graphitic
Nickel-iron (1 : 1)	530	Highly graphitic
Ruthenium	535	Highly graphitic
Iridium	965	Amorphous
Platinum-iridium (1 : 1)	850	Amorphous

[a]Spreading temperature is defined as the point where particles undergo transition from wetting to spreading, as depicted in Fig. 4.
[b]Produced by the interaction of the metal with ethylene/hydrogen at temperature between 500 and 650 °C.

weaker interaction with graphite and produce nanofiber structures that contain a large fraction of amorphous carbon. On the other hand, when either copper or iron is mixed with nickel, then there is a significant increase in the wetting characteristics with respect to graphite and such catalyst particles tend to generate highly ordered carbon nanostructures.[88,89] In this regard, the copper-nickel system is extremely interesting since it is possible to control the chemical nature of the filaments merely by altering the ratio of the alloy constituent; particles rich in nickel were found to produce much more ordered filament structures than those grown from either pure nickel or copper-rich particles.[61]

E. Factors controlling the diameter of carbon nanofibers

The selection of the form of the catalyst (supported or unsupported) and the temperature at which the reaction is conducted influence the size of the metal particles and this latter parameter is ultimately responsible for determining the diameter of the carbon nanofibers produced when the metal is reacted in the presence of an appropriate carbon-containing gas. If the starting material is either a metal foil or powder, then the widths of the nanostructures are found to vary over a wide range and are somewhat unpredictable. It has also been found that the diameter of the nanofibers is governed by the size of the associated catalyst particles and varies from 25 to 100 nm when the starting material was a metal powder.[47] In this case, it was evident that the active particles were considerably smaller than those of the original metal powders (~1 μm average diameter) which suggested that during reaction fragmentation of the starting material occurred prior to the creation of the carbon nanofibers. Fragmentation of metal particles during carbon deposition was proposed by Guinot and coworkers[90] to explain the relatively high rates of reaction of samples with low specific surface area. The phenomenon of "surface breakup" was also suggested by Jablonski and coworkers[91] as a necessary step in the formation of carbon nanofibers on metal foils undergoing reaction with carbon monoxide mixtures.

If one desires to produce carbon nanofibers in a well-controlled size range, then the preferred route is to use a supported metal particle arrangement. Such a sample can be produced by depositing a few monolayers of the catalytically active metal onto a carrier material such as carbon, alumina, or silica followed by nucleation to form small particles.[92] Subsequent reaction of these samples in a suitable carbon-containing gas environment will result in the formation of carbon nanostructures having the same diameter as those of the starting metal catalyst particles.[12,14] This approach also lends a degree of flexibility for the choice of the range of widths of the carbon nanofibers, since factors such as the strength of the metal-support interaction and the reaction temperature have a direct impact on the ultimate size of the dispersed catalyst particle. Other methods have been proposed by Endo and coworkers[30,32] to produce carbon nanofibers of smaller diameters, involving the use of organic or inorganic iron compound solutions which are subsequently sprayed onto a substrate.

Some interesting features can be seen from the data presented in Figs. 5 and 6, which show the change in the size ranges of carbon nanofibers produced from the interaction of identical loadings of cobalt particles supported on graphite and amorphous carbon, respectively, with ethylene-hydrogen (4 : 1) as a function of reaction

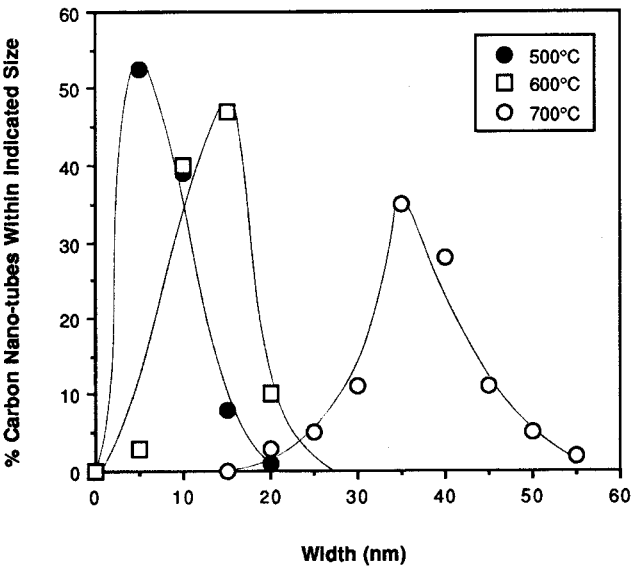

FIG. 5. Carbon nanofiber width distributions produced from the interaction of cobalt/graphite specimens with ethylene/hydrogen (4 : 1) as a function of reaction temperature.

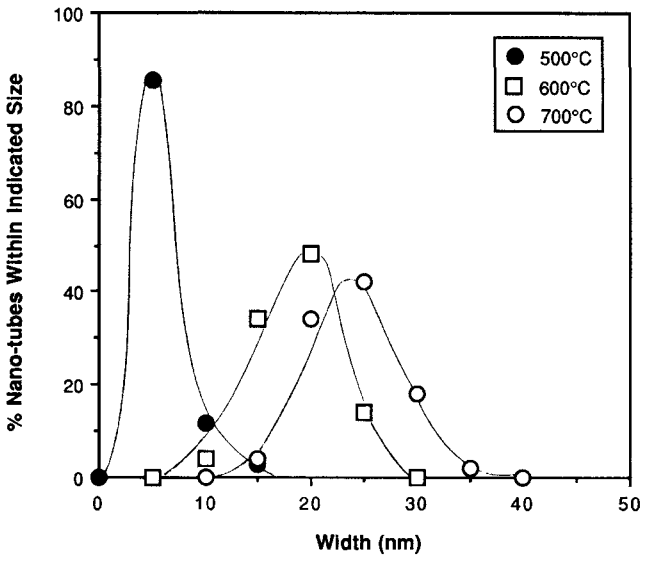

FIG. 6. Carbon nanofiber width distributions produced from the interaction of cobalt/amorphous carbon specimens with ethylene/hydrogen (4 : 1) as a function of reaction temperature.

temperature. It is evident that significant differences exist between the behavior of cobalt on these two types of carbonaceous supports, which has ramifications on the ultimate width of the carbon nanofibers produced when the catalyst particles were reacted in the ethylene-hydrogen mixture. In general, cobalt particle growth is more constrained on amorphous carbon than graphite, and as a consequence there is a tendency for the creation of both a smaller average size and a narrower size range distribution of carbon nanofibers to be formed from cobalt/carbon than from cobalt/graphite samples. One exception to this trend is found for the samples treated at 600 °C, a condition where it is known that cobalt exhibits a strong interaction with graphite edge atoms which results in discrete particles undergoing a spreading action to form a thin film along these regions.[82] This transformation leads to the rupture of large particles into smaller ones, a process that is commonly referred to as "redispersion". Under such circumstances, it is therefore not surprising to find that at 600 °C the average width of the carbon nanofibers formed on cobalt/graphite samples is significantly smaller than those grown from cobalt/amorphous carbon at the same temperature.

If there is a need to produce the nanostructures in a relatively small size range at temperatures of ~700 °C, then one might select a system in which cobalt exhibits a very strong metal/support interaction and as a consequence limited sintering behavior. A support medium that would most likely satisfy these requirements is γ-alumina.[93]

IV. CHEMICAL AND PHYSICAL PROPERTIES OF CARBON NANOFIBERS

A. Structural characterization studies

Controlled oxidation experiments performed within the electron microscope revealed that carbon nanofibers produced from the interaction of iron, cobalt, and nickel particles with acetylene at temperatures between 600 and 700 °C consisted of a duplex structure, an inner core of amorphous carbon surrounded by a skin of graphitic platelets.[12,14] In more recent years, it has been found that the internal structural arrangement of the carbon nanofibers can be significantly different from that described above, and is extremely sensitive to a number of factors, particularly the chemical nature of the catalyst and the composition of the gaseous reactant.

Improvements in the procedure relating to the growth on nanofibers now enable one to produce sizable quantities of the material, and this accomplishment has opened up the possibility of using bulk methods to characterize the structures. The behavioral pattern accompanying the controlled oxidation of carbonaceous solids in CO_2 provides a very sensitive means of determining the degree of structural perfection of such materials. These experiments are carried out in a Cahn 2000 micro-balance in which the temperature of the reactor can be programmed up to 1000 °C at a constant heating rate of the order of 5 °C/min. The weight loss is then recorded as a function of temperature and time. The tactic is to compare the reactivity of the catalytically produced carbon nanofibers with that of two forms of carbon that possess extreme structural order: graphite (highly crystalline material) and active carbon (amorphous in nature) containing the same loading of metal catalyst. In most cases it is possible to remove the metal catalyst from the carbon nanostructures and therefore there is no need to introduce such species onto the reference materials. From these experiments it is possible to obtain a measure of the relative amounts of graphite and amorphous carbon in a given batch of carbon nanofibers. Other workers[94] have attempted to characterize these types of carbon structures by following their reactivity toward hydrogen. In this case, however, the analysis was limited to the determination of methane yields with no effort apparently being made to ascertain the corresponding loss in weight of the solid sample.

An example of the data obtained from the use of this approach is shown in Fig. 7 for carbon nanofibers produced from the platinum catalyzed decomposition of 10% acetylene-hydrogen and 30% ethylene-hydrogen mixtures, respectively.[77] Also included in this plot for reference purposes are the oxidation profiles of 5% Pt/graphite and 5% Pt/amorphous carbon samples. It can be seen that the latter sample starts to react at 550 °C and

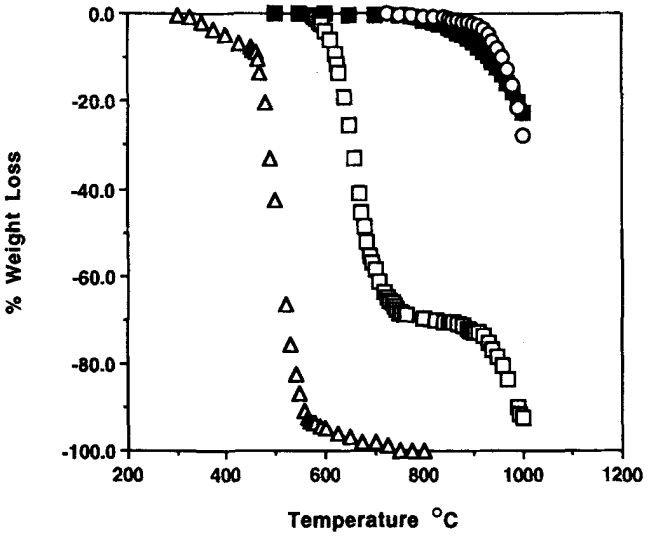

FIG. 7. Temperature programmed oxidation in CO_2 of carbon nanofibers produced from the decomposition of hydrocarbon-hydrogen mixtures over platinum as compared to graphite and amorphous carbon impregnated with an equivalent amount of catalyst: (○) nanofibers from 36% C_2H_2/H_2; (□) nanofibers from 8% C_2H_4/H_2; (△) amorphous carbon; (■) graphite (Ref. 77 with permission).

is essentially completely gasified at 750 °C. In contrast, the onset of gasification of the graphite sample occurs at 800 °C and 75% of the material is still present at 1000 °C. A correlation of the thermograms obtained from the two carbon deposit samples with those of the reference materials shows that the nanofibers produced from the platinum-ethylene-hydrogen mixture consist of a duplex structure, a large fraction of amorphous carbon combined with a smaller amount of graphite. On the other hand, when acetylene is used as the source of carbon, then the nanostructures are entirely graphitic in nature.

When controlled atmosphere electron microscopy was used to follow the interaction of carbon nanofibers with oxygen, it was possible to gain some unique insights into the structural characteristics of the material. In cases where the nanostructures had been produced from the decomposition of acetylene over iron, cobalt, and nickel, it was found that the inner portions started to oxidize at ~600 °C, leaving behind a relatively oxidation resistant outer region.[12,14] This stage in the reaction can be seen in the electron micrograph, Fig. 8, which shows the appearance of hollow nanofibers formed during exposure to 5 Torr oxygen at 600 °C. On removal of the amorphous core component, the presence of small metal particles (2–20 nm diameter) was revealed which appeared to be present as inclusions in the graphitic skin. These particles were clearly distinguishable from those that remained on the support, as they moved with the oscillating motion of the nanofibers in which they were embedded.

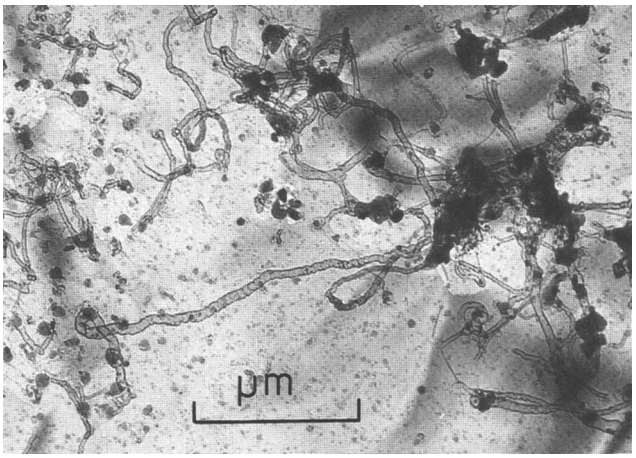

FIG. 8. Transmission electron micrograph of partially oxidized carbon nanofibers (note the appearance of small metallic inclusions in some of the structures) (reprinted with permission from Academic Press, Ref. 95).

This observation suggests that during the growth cycle under certain circumstances material can be lost from the catalyst particle and effectively dispersed throughout the solid carbon structure. If the oxidation reaction was continued, then at about 725 °C complete removal of the graphitic skin was achieved, leaving a skeletal arrangement of the small metal particles.[95] In further controlled oxidation studies it was found that when carbon nanofibers produced from the iron catalyzed, decomposition of $CO-H_2$ mixtures was subsequently reacted in oxygen, the structures consisting of a single component, which underwent reaction at an identical rate to that of the single crystal graphite on which they were supported.[96]

An equally fascinating study carried out with the same technique was the discovery that nickel could catalyze the growth of carbon nanofibers in the presence of acetylene and also promote their removal when the hydrocarbon was replaced with hydrogen[27]; moreover, in subsequent cycling experiments between these two gases, it was found that the carbon formation and hydrogasification steps were completely reversible. Detailed kinetic analysis of several sequences showed that carbon diffusion through the catalyst particle was a common step in both processes; in one case, the fate of the carbon being the formation of a solid nanostructure and in the other, the carbon being converted into methane.

The more traditional techniques such as transmission electron microscopy coupled with electron diffraction and x-ray diffraction have revealed some of the more intimate details regarding the alignment and dimensions of the graphite crystallite component. The average thickness of the stacks of parallel graphitic layers, designated L_c, existing within the carbon nanofibers can be estimated from broadening of the principal peaks ($00l$) obtained

from a given sample.[97] Although the diffraction techniques are more sensitive than the controlled oxidation approach for the detection of graphitic carbon, they do not allow one to determine the relative amounts of graphite to amorphous carbon present in the nanofibers.

Table III shows the crystallite thickness, L_c (nm), obtained from carbon nanofibers formed from nickel and nickel pre-sulfided at various levels prior to reaction in an ethylene/hydrogen (1 : 4) mixture at 600 °C.[98] X-ray diffraction measurements were carried out in a Rigaku Geigerflex DMAX B diffractometer using Cu K_α with a graphite monochromator. The scan rate of 15°/min was used for the 2Θ range of 20 to 150°. Inspection of these data shows that pretreatment of nickel in a sulfur containing environment has a dramatic effect on the thickness of the graphite crystallite stacks contained in the nanofiber structures, which indicates that sulfur exerts an influence on the behavior of nickel atoms at the metal/solid carbon interface, as well as plays a role in dictating the chemistry occurring at the front face of the catalyst particle.

High resolution transmission electron microscopy studies of individual nanofibers gives direct information pertaining to the dimensions and arrangement of the graphitic crystallites with respect to both the fiber axis and the facets that exist at the rear of the metal particle. Further information regarding the structural characteristics can be obtained from selected area electron diffraction patterns, an aspect that has been studied in great detail by several groups.[3,21,37,99]

In summary, it is apparent that by judicious choice of the catalyst, the ratio of the hydrocarbon-hydrogen reaction mixture, and the reaction temperature, it is possible to tailor the morphological characteristics, the degree of crystallinity, and the orientation of the graphite crystallites with respect to the fiber axis. Indeed, it has been possible to produce carbon nanofibers that are entirely graphitic in nature at temperatures as low as 550 °C.[77,78]

B. Adsorption characteristics of carbon nanofibers

Because of the potential of catalytically grown carbon nanofibers in a variety of innovative technologies including energy storage devices as well as cleaning of the environment, surface area and adsorption properties are of extreme importance. When adsorption of nitrogen at −196 °C was used for the determination of surface area, the typical curve obtained from the uptake of N_2 on carbon nanofibers produced from the copper-nickel catalyzed decomposition of ethylene followed the shape shown in Fig. 9 and corresponds to a Type II isotherm, typical of a nonporous solid or with porosity inaccessible to nitrogen.[100] Surface areas were calculated from the BET equation and found to be dependent on a combination of parameters such as gas composition, temperature, and chemical nature of the catalyst. The variation of surface area with catalyst composition is presented in Fig. 10 for a selection of carbon nanofibers obtained from the decomposition of ethylene-hydrogen over Cu–Ni powders at 600 °C. The values range from ~10 m^2/g for material obtained using copper-rich powders to ~250 m^2/g for powdered catalyst precursors containing a large fraction of nickel and decreases to about 75 m^2/g for carbon nanofibers formed from pure nickel.[101] Copper does not catalyze the growth of this type of structure since it is unable to decompose hydrocarbons. The effect of both gas composition and addition of nonmetallic adatoms to the surface of the metal catalyst particle also influences the value of the surface area of carbon nanofibers, and an example of such interdependence is presented in Table IV. Pretreatment of nickel with H_2S resulted in an increase in the surface area from 107 m^2/g for untreated catalyst to 363 m^2/g following pre-sulfidization of the catalyst in 50 ppm H_2S.[98] It is also apparent from Table IV that the reactant gas composition has an impact on the surface area of the carbon nanostructures, the presence of large amounts of hydrogen in the feed generating structures with relatively large surface areas. A further parameter which must be taken into consideration with regard to the surface area

TABLE III. Effect of sulfur pretreatment on the crystallinity of carbon nanofibers produced from the decomposition of ethylene-hydrogen over nickel at 600 °C.[98]

Pretreatment, ppm H_2S	L_c (nm)
None	9.22
4	8.62
16	8.55
50	6.89

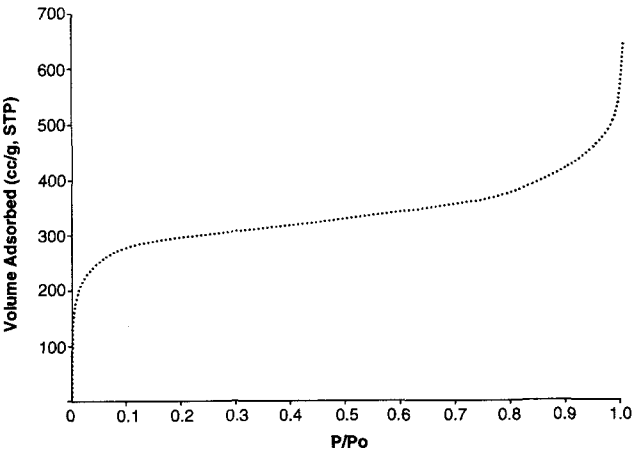

FIG. 9. Adsorption isotherm of nitrogen on carbon nanofibers at −196 °C (Ref. 101 with permission).

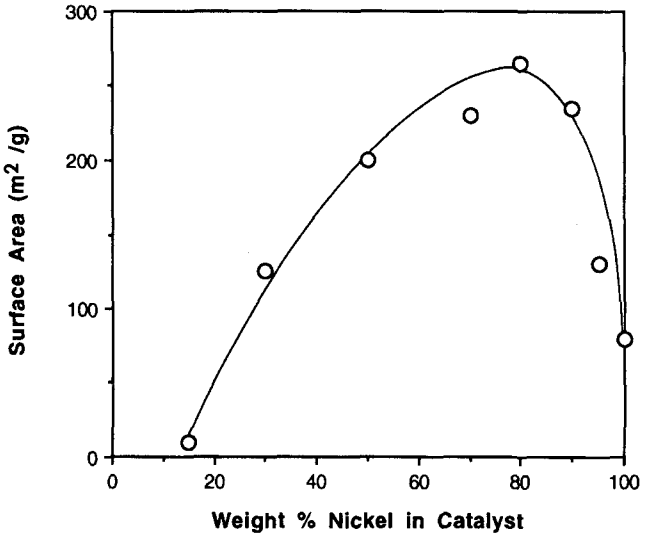

FIG. 10. Variation of surface area of carbon nanofibers as a function of catalyst composition (Ref. 101 with permission).

of carbon nanofibers is the temperature at which they are produced.

It is clear that the variation in surface area is extremely sensitive to the conditions under which carbon nanofibers are grown, and it is certainly associated with not only the overall crystallinity but also the manner in which individual graphite crystallites within the structure are aligned with respect to each other. As pointed out previously, many of the physical properties of carbon nanofibers are dictated by nature of the metal/carbon interaction and, in particular, the crystallographic faces of the particle present at the interface with the solid carbon structure. Modifications in the structural arrangements of the nanofibers can result from the introduction of adatoms, both metal and nonmetals, and the pretreatment of the catalyst system, in particular gas environments, which can induce reconstruction of metal crystallite faces. A further aspect that should be taken into consideration is the influence of hydrogen, which is commonly present in the reactant mixture, on the structural perfection of the carbon nanofiber.

The potential of carbon nanofibers as an adsorbent in aqueous solutions was examined by the adsorption of iodine from a I_2/KI solution,[102] following the procedure reported by Meguro and coworkers,[103] who demonstrated that in such a solution only I_2 was selectively adsorbed. The uptake of I_2 on carbon nanofibers followed a type I (Langmuir) isotherm [100], which is characteristic of monolayer adsorption, and this behavior is illustrated in Fig. 11. The apparent surface area obtained from this approach was 350 m^2/g, a much higher value than that obtained from adsorption of nitrogen (~250 m^2/g); however, one must take into account that in this case in addition to physical adsorption there may also be a contribution from chemical effects such as the possible formation of charge transfer complexes. The adsorption of I_2 from aqueous solutions has been used previously to study structural parameters of various carbonaceous solids,[104] and it was established that the interaction was extremely dependent on the chemical nature of the solid carbon, particularly with regard to polarity. I_2 is known to form charge transfer complexes with condensed polynuclear aromatic hydrocarbons and is therefore expected to establish a very strong interaction with the graphitic crystallites that are present in the carbon nanofibers.

TABLE IV. Effect of gas composition and sulfur pretreatment on the surface area of carbon nanofibers produced from the decomposition of ethylene-hydrogen over nickel at 600 °C.[98]

Pretreatment ppm H_2S	Ethylene-hydrogen ratio		
	1:0	4:1	1:4
None	...	107.9	107.8
16	114.7	117.2	203.9
50	122.6	135.1	363.8

C. Density

The combination of structural parameters and variable conformations of catalytically grown carbon nanofibers offers the potential of using the material in reinforcement applications where the density is a critical factor. The density of a series of carbons was determined by suspension of a small sample in mixtures of carbon tetrachloride and tetrabromoethane with known density.[105] Catalyst particles that might have

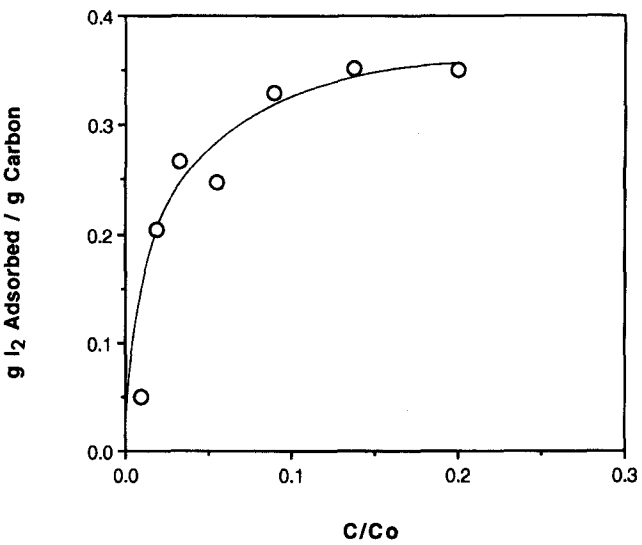

FIG. 11. Adsorption isotherm of iodine on carbon nanofibers at 25 °C. C is the concentration of the I_2 solution in contact with the adsorbent and C_0 is the concentration of I_2 in saturated solution.

been present were removed prior to the determination by immersion of the samples in a dilute solution of HCl for three days, followed by exhaustive washing and vacuum drying. TEM examination of the samples after such treatment indicated that no visible changes in structure had occurred. The measured values of density for carbon nanofibers obtained from the decomposition of ethylene over various copper-nickel alloys are presented in Fig. 12 where it can be seen that the density increases in a relatively smooth fashion as the nickel content of the catalyst particle is increased.

D. Mechanical properties of carbon nanofibers

The information available on the mechanical properties of individual carbon nanofibers is extremely limited due to the difficulties in manipulating such minute structures. A recent paper by Motojima and coworkers[17] describes some very elegant experiments for the examination of the elastic properties of relatively large-sized coiled carbon nanostructures. In this study, one end of the nanofiber was fixed to a copper mesh with an adhesive and the other end pulled in order to extend the coiled structure. From the observations conducted in the transmission electron microscope it was possible to determine the extension ratio as a function of the original coil length. They found that the structures could be extended elastically up to 3.0 times their original length and semielastically up to 4.5 times.

In another investigation[106] carbon nanofibers were grown on the side of conventional carbon fibers and the change in interfacial properties realized by this treatment over pristine fibers was determined by the tensile bar technique. In this approach single fibers were embedded in a thin layer of matrix which was then affixed to a suitable aluminum bar. The bar was subsequently strained so that stress was transferred to the fiber through the matrix until the fiber eventually broke into small fragments. This test was based on the principle that the stronger the interfacial interaction between the fiber and matrix, then the shorter would be the fractured segments. Using these measurements it was possible to calculate the frictional shear stress of a given fiber. From the data obtained by this method it was found that a 450% increase in interlaminar shear strength could be achieved when T300 carbon fibers were loaded with a 1 wt. % of catalyst and subsequently treated in ethylene/hydrogen for 2 h. It was also significant that the reaction leading to the growth of carbon nanofibers did not induce any weakening of the parent fiber, since tensile strength measurements on specimens that had been in the reactor for 2 h were identical to those obtained on untreated fibers.

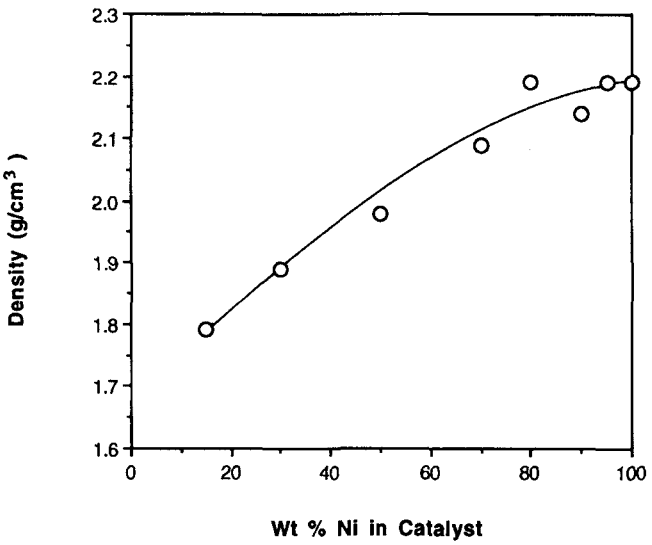

FIG. 12. Relationship between the density of carbon nanofibers produced from the decomposition of ethylene at 600 °C and the composition of the catalyst.

E. Electrical properties of carbon nanofibers

The unique crystalline arrangement encountered in carbon nanofibers, which is controlled by the atomic arrangement of the catalyst particle surface in contact with the solid carbon, suggests that the material will possess certain electrical properties associated with the preparation conditions. Due to the extremely small size of the material, direct determination of electrical resistivity could not be accomplished by conventional methods. In order to overcome this difficulty, a device was built that allowed the measurement of resistivity of powdered materials while the sample was held under a constant pressure.[101] The apparatus consisted of a hollow cylinder which was internally lined with a nonconductive ceramic sleeve in which two brass pistons formed a pressure chamber.[107] The two-probe electrical resistance across the sample was measured using a 3465B Hewlett Packard Digital Multimeter while the sample was under 9000 psi pressure. The height of the sample bed was determined using a micrometer and the apparatus calibrated using standard carbon materials with known electrical resistivity. The results of the measurements for a series of carbon nanofibers are presented in Fig. 13. It should be appreciated that the data reported for the electrical resistivities of the carbon nanofibers may be much higher than the real values because of the presence of voids within the sample.

V. POTENTIAL APPLICATIONS

A. Carbon nanofibers as catalysts and catalyst supports

It has been demonstrated that a variety of carbonaceous materials including carbon fibers are capable of transforming mixtures of NO and NH_3 into N_2 and H_2;

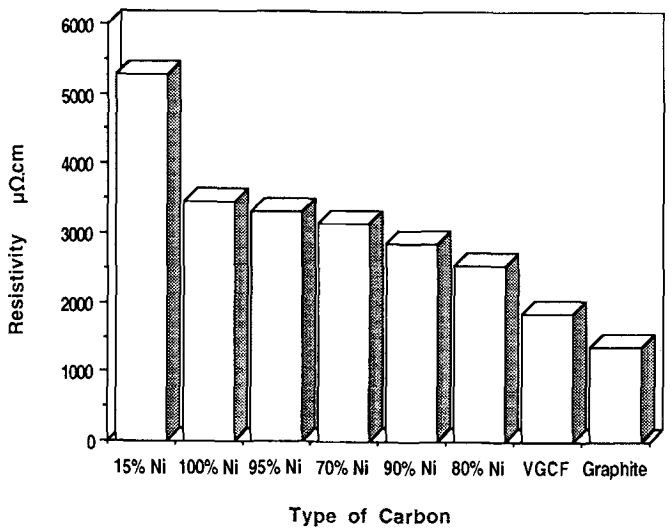

FIG. 13. Comparison of the electrical resistivities of carbon nanofibers from various preparations compared to those of vapor grown carbon fibers (VGCF) (from Ref. 4, p. 196) and graphite.

however, the reaction is inhibited by the presence of small amounts of water, and this feature has prompted the search for materials that can exhibit hydrophobic behavior as well as high surface area.[108–110] When used as catalyst support media, carbon nanofibers offer some unique advantages over the more traditional materials such as alumina or silica since the former material not only exhibits high surface areas but is also an electrical conductor. Therefore, there is the possibility that metal crystallites introduced onto carbon nanofibers will form very strong interactions with the surface and as a consequence modifications in the morphological characteristics of the catalyst particles could give rise to unexpected activity and selectivity patterns.[111,112] It is this combination of structural and electrical properties that make carbon nanofibers a very attractive candidate for exploitation both as a catalyst and a catalyst support medium.

B. Selective adsorption agents

The pore structure of carbon nanofibers is ideal for rapid adsorption/desorption of a large amount of gas since their thin fiber form provides a large number of shallow pores in the surface regions.[101] In addition, different surface treatments of the nanofiber surfaces can produce a variety of functional groups and this aspect presents some interesting opportunities for the utilization of the material in pollution control applications. Since carbon nanofibers exhibit a very high mechanical strength,[113] there is the potential to use the material in liquid phase reactions as they not only withstand vigorous agitation, but also provide improved transport properties over that found with more conventional adsorbents.

C. Use of carbon nanofibers in reinforcement

In general, the performance of a fibrous composite depends not only on the properties of the components, but also to a large degree on the coupling between the fiber and the matrix. In order to increase the interlaminar shear strength, numerous attempts have been made to improve bonding between the fiber and the matrix, consisting mostly of chemical and physical modifications to the fiber surface.[114,115] One approach has involved etching of the fiber surfaces by treatment in conventional oxidizing agents,[116,117] which causes roughening of the structure thereby increasing the surface area and enhancing the mechanical link with the matrix. More recently, plasma etching[118] and reaction in atomic oxygen[119,120] have been used to increase the surface area of the fibers by producing micropits in the surface of the carbon structures. Although these chemical treatments do improve the bonding of the fiber to the matrix, they must be applied under well-controlled conditions, otherwise such reactions can lead to extensive damage and weakening of the structure.[120]

A novel approach was the notion of growing carbon nanofibers on the surface of conventional carbon fibers via carbon vapor deposition in the presence of a minuscule amount of metal catalyst.[48,49] The presence of the carbon nanostructures on the carbon fiber surface was found to enhance the surface area of the preform from ~2 m^2/g up to over 400 m^2/g and consequently increased the interfacial bonding between the fiber and the matrix. This improvement was achieved without causing a concomitant degradation of the carbon fiber structure. Figure 14 is a scanning electron micrograph showing the formation of carbon nanofibers on the surfaces of a bundle of T-300 carbon fibers.[48]

It is well established that in order for a fiber to function successfully as reinforcement in high-

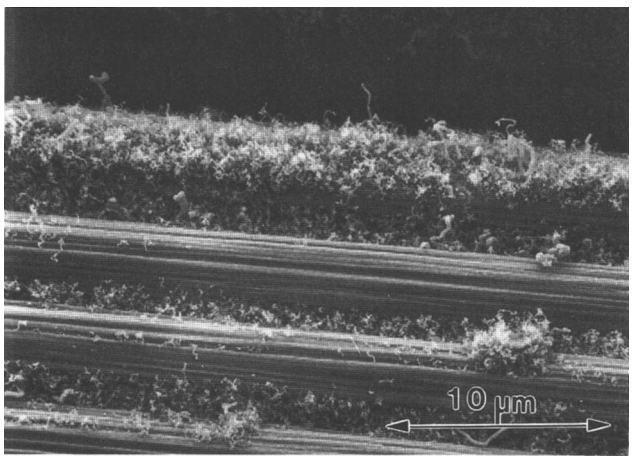

FIG. 14. Scanning electron micrograph showing the growth of carbon nanofibers on the surface of a bundle of a T300 carbon fiber (reprinted with permission from Pergamon Press, Ref. 48).

performance engineering materials, it must fulfill certain criteria:[115,121,122]

(i) A small diameter with respect to its grain size is needed since there will be a low probability of intrinsic imperfections in the material and experimental evidence shows that the strength of the fiber increases as its diameter decreases.[123] In this regard, catalytically grown carbon nanofibers would appear to be superior to other types of carbon fibers since their diameters, which are controlled by the size of the catalyst particles responsible for producing them, can be as low as 2 nm.

(ii) A high aspect ratio is needed which ensures that a very large fraction of the applied load will be transferred through the matrix to the stiff and strong fiber. In general, carbon nanofibers possess extremely small diameters and high aspect ratios, typically ~150.

(iii) A very high degree of flexibility is desirable for the complex series of operations involved in composite fabrication. As mentioned previously, when carbon nanofibers are produced in a helical conformation they were found to possess appreciable elastic properties.

From the foregoing discussion it is clear that because of the exceptional properties exhibited by catalytically produced carbon nanofibers, such a material has a tremendous potential for reinforcement applications in its own right.

D. Use of carbon nanofibers in energy storage devices

The operation of electric double layer capacitors is based on a phenomenon at the interface between an ionic conductive electrolyte and an electrically conductive high surface area electrode.[124,125] Sulfuric acid solution and activated carbon are generally the electrolyte and electrode, respectively. Although activated carbon possesses a very high surface area (~1000 m^2/g), due to structural parameters its electrical conductivity is very poor. The replacement of activated carbon by other materials that combine a relatively high surface area with a high electrical conductivity could produce a remarkable improvement in the system. In this regard, the catalytically grown carbon nanofibers would appear to be a very attractive material for the capacitor electrode, since it has a high surface area (~700 m^2/g when activated) and electrical conductivity very close to that of pure graphite. The viability of using carbon nanofibers as electrodes for energy storage devices has been demonstrated by Matsumoto and coworkers[126] who found that the performance of partially oxidized carbon nanofibers was superior to that of activated continuous carbon fibers and this aspect was believed to be related to structural parameters and in particular, the higher electrical conductivity of the former material.

ACKNOWLEDGMENTS

The author would like to thank Professor R. Terry K. Baker for stimulating discussions and encouragement during the preparation of this manuscript and Dr. Myung-Soo Kim for help with some of the experiments. Financial support for this work was provided by the National Science Foundation, Grant Nos. NSF-MSS-8902939-A and CBT-8800931, and the Department of Energy, Basic Energy Sciences, Grant DE-FG05-89ER14076.

REFERENCES

1. S. Iijima, Nature **354**, 56 (1991).
2. R. T. K. Baker and P. S. Harris, in *Chemistry and Physics of Carbon,* edited by P. L. Walker, Jr. and P. A. Thrower (Marcel Dekker, New York, 1978), Vol. 14, p. 83.
3. A. Oberlin, M. Endo, and T. Koyama, J. Cryst. Growth **32**, 335 (1976).
4. M. S. Dresselhaus, G. Dresselhaus, K. Sugihara, I. L. Spain, and H. A. Goldberg, *Graphite Fibers and Filaments,* Springer Series in Materials Science 5 (Springer-Verlag, New York, 1988).
5. *Carbon Fibers, Filaments and Composites,* edited by J. L. Figueiredo, C. A. Bernardo, R. T. K. Baker, and K. J. Huttinger, NATO ASI Series (Kluwer Academic Publishers, Dordrecht, The Netherlands, 1989), Vol. 177, pp. 405, 562.
6. P. Schutzenberger, C.R. Acad. Sci. Paris **111**, 774 (1980).
7. J. R. Rostrup-Nielsen, *Steam Reforming Catalysts,* Tekorisk Forlay A/S (Danish Technical Press, Copenhagen, 1975).
8. D. L. Trimm, Catal. Rev.-Sci. Eng. **16**, 155 (1977).
9. *Coke Formation on Metal Surfaces,* edited by L. F. Albright and R. T. K. Baker, ACS Symposium Series 202 (1982).
10. M. J. Bennett and J. B. Price, J. Mater. Sci. **16**, 170 (1981).
11. C. H. Bartholomew, Catal. Rev.-Sci. Eng. **24**, 67 (1982).
12. R. T. K. Baker, M. A. Barber, P. S. Harris, F. S. Feates, and R. J. Waite, J. Catal. **26**, 51 (1972).
13. R. T. K. Baker, S. Terry, and P. S. Harris, Nature **253**, 37 (1975).
14. R. T. K. Baker, P. S. Harris, R. B. Thomas, and R. J. Waite, J. Catal. **30**, 86 (1973).
15. H. P. Boehm, Carbon **11**, 583 (1973).
16. M. T. Tavares, C. A. Bernardo, I. Alstrup, and J. R. Rostrup-Nielsen, J. Catal. **100**, 545 (1986).
17. S. Motojima, M. Kawaguchi, K. Nozaki, and H. Iwanaga, Carbon **29**, 379 (1991).
18. T. Baird, J. R. Fryer, and B. Grant, Nature **233**, 329 (1971).
19. M. Audier, A. Oberlin, and M. Coulon, J. Cryst. Growth **55**, 549 (1981).
20. E. Boellaard, P. K. DeBokx, A. J. H. M. Kock, and J. W. Geus, J. Catal. **96**, 481 (1985).
21. M. Raghavan, Proc. 37th Annual EMSA Meeting, edited by G. W. Bailey, p. 484.
22. M. Audier, A. Oberlin, M. Oberlin, M. Coulon, and L. Bonnetain, Carbon **19**, 217 (1981).
23. G. G. Tibbetts, J. Cryst. Growth **66**, 632 (1984).
24. R. T. Yang and J. P. Chen, J. Catal. **115**, 52 (1989).
25. D. W. Goodman, R. D. Kelley, T. E. Madey, and J. T. Yates, Jr., J. Catal. **63**, 226 (1980).
26. J. Nakamura, H. Hirano, M. Xie, I. Matsuo, T. Yamada, and K. Tanaka, Surf. Sci. **222**, L809 (1989).
27. J. L. Figueiredo, C. A. Bernardo, J. J. Chludzinski, and R. T. K. Baker, J. Catal. **110**, 127 (1988).
28. T. Koyama, Carbon **10**, 757 (1972).

29. T. Koyama, M. Endo, and Y. Onuma, Jpn. J. Appl. Phys. **11**, 445 (1972).
30. T. Koyama and M. Endo, Jpn. J. Appl. Phys. **13**, 1175 (1974).
31. M. Endo, T. Koyama, and Y. Hishiyama, Jpn. J. Appl. Phys. **15**, 2073 (1976).
32. M. Endo, M. Shikata, T. Momose, and M. Shiraishi, Proc. 17th Biennial Conf. on Carbon, 297 (1985).
33. M. Endo, H. Yamanashi, and G.L. Doll, J. Appl. Phys. **64**, 2995 (1988).
34. G.G. Tibbetts, Appl. Phys. Lett. **42**, 666 (1983).
35. J.R. Bradley and G.G. Tibbetts, Carbon **23**, 423 (1985).
36. G.G. Tibbetts, M.G. DeVour, and E.J. Rodda, Carbon **25**, 367 (1987).
37. F. Benissad, P. Gadelle, M. Coulon, and L. Bonnetain, Carbon **26**, 61 (1988).
38. F. Benissad, P. Gadelle, M. Coulon, and L. Bonnetain, Carbon **26**, 425 (1988).
39. G.G. Tibbetts and E.J. Rodda, in *Microstructures and Properties of Catalysts,* edited by M.M.J. Treacy, J.M. Thomas, and J.M. White (Mater. Res. Soc. Symp. Proc. **111**, Pittsburgh, PA, 1988), p. 49.
40. F. Benissad, P. Gadelle, M. Coulon, and L. Bonnetain, Carbon **27**, 585 (1989).
41. M. Ishioka, T. Okada, K. Matsubara, and M. Endo, Carbon **30**, 859 (1992).
42. M. Ishioka, T. Okada, K. Matsubara, and M. Endo, Carbon **30**, 865 (1992).
43. G.G. Tibbetts, Carbon **30**, 399 (1992).
44. M. Ishioka, T. Okada, and K. Matsubara, Carbon **30**, 975 (1992).
45. T. Kato, K. Haruta, K. Kusakabe, and S. Morooka, Carbon **30**, 989 (1992).
46. T. Masuda, S.R. Mukai, and K. Hashimoto, Carbon **30**, 124 (1992).
47. M.S. Kim, N.M. Rodriguez, and R.T.K. Baker, J. Catal. **131**, 60 (1991).
48. W.B. Downs and R.T.K. Baker, Carbon **29**, 1173 (1991).
49. P. McAllister and E.E. Wolf, Carbon **30**, 189 (1992).
50. R.T.K. Baker, in *Carbon and Coal Gasification,* edited by J.L. Figueiredo and J.A. Moulijn, NATO ASI Series 105 (Martinus Nijhoff Publishers, Dordrecht, The Netherlands, 1986), p. 231.
51. J.R. Rostrup-Nielsen, J. Catal. **27**, 343 (1972).
52. L.S. Lobo and D.L. Trimm, J. Catal. **29**, 15 (1973).
53. C.A. Bernardo and L.S. Lobo, J. Catal. **37**, 267 (1975).
54. J.R. Rostrup-Nielsen and D.L. Trimm, J. Catal. **48**, 155 (1977).
55. R.T. Yang and K.L. Yang, J. Catal. **93**, 182 (1985).
56. A. Sacco, P. Thacker, T.N. Chang, and A.T.S. Chiang, J. Catal. **85**, 224 (1984).
57. A.J.H.M. Kock, P.K. de Bokx, E. Boellaard, W. Klop, and J.W. Geus, J. Catal. **96**, 468 (1985).
58. I. Alstrup, J. Catal. **109**, 241 (1988).
59. S.A. Safvi, E.C. Bianchini, and C.R.F. Lund, Carbon **29**, 1245 (1991).
60. P. Chitrapu, C.R.F. Lund, and J.A. Tsamopoulos, Carbon **30**, 285 (1992).
61. M.S. Kim, N.M. Rodriguez, and R.T.K. Baker, J. Catal. **134**, 253 (1991).
62. M. Audier, J. Guinot, M. Coulon, and L. Bonnetain, Carbon **19**, 99 (1981).
63. R.T.K. Baker and J.J. Chludzinski, J. Catal. **64**, 464 (1980).
64. R.J. Koestner, J.C. Frost, P.C. Stair, M.A. Van Hove, and G.A. Somorjai, Surf. Sci. **116**, 85 (1982).
65. X.Y. Zhu and J.M. White, Surf. Sci. **214**, 240 (1989).
66. M.A. Barteau, E.J. Ko, and R.J. Madix, Surf. Sci. **102**, 99 (1981).
67. E. Yagasaki and R.I. Masel, Surf. Sci. **226**, 51 (1990).
68. W.H. Wienberg, R.P. Deans, and R.P. Merrill, Surf. Sci. **41**, 312 (1974).
69. R.C. Baetzold, Surf. Sci. **95**, 286 (1980).
70. R.J. Koestner, M.A. Van Hove, and G.A. Somorjai, Chem. Tech. **13**, 376 (1983).
71. J. Nakamura, I. Toyoshima, and K. Tanaka, Surf. Sci. **201**, 185 (1988).
72. R.B. White, U.S. Patent 2 621 216.
73. D.C. Gardner and C.H. Bartholomew, Ind. Eng. Chem. Prod. Res. Dev. **20**, 80 (1981).
74. B. Lang, Surf. Sci. **53**, 317 (1975).
75. S. Hagstrem, H.B. Lyon, and G.A. Somorjai, Phys. Rev. Lett. **15**, 491 (1975).
76. H.P. Bonzel and R. Ku, Surf. Sci. **33**, 91 (1972).
77. W.T. Owens, N.M. Rodriguez, and R.T.K. Baker, J. Phys. Chem. **96**, 5048 (1992).
78. M.S. Kim, N.M. Rodriguez, and R.T.K. Baker, J. Catal. (in press).
79. M. Audier, P. Bowen, and W. Jones, J. Cryst. Growth **64**, 291 (1983).
80. R.T.K. Baker, J.R. Alonzo, J.A. Dumesic, and D.J.C. Yates, J. Catal. **77**, 74 (1982).
81. K.L. Yang and R.T. Yang, Carbon **24**, 687 (1986).
82. S.G. Oh and R.T.K. Baker, J. Catal. **128**, 137 (1991).
83. N.M. Rodriguez, M.S. Kim, and R.T.K. Baker, J. Catal. **140**, 16 (1993).
84. J.G. McCarty, P.Y. Hou, D. Sheridan, and H. Wise, in *Coke Formation on Metal Surfaces,* edited by L.F. Albright and R.T.K. Baker, ACS Symposium Series 202, 252 (1981).
85. M. Audier, A. Oberlin, and M. Coulon, J. Cryst. Growth **55**, 549 (1981).
86. M. Humenik and W.D. Kingery, J. Am. Ceram. Soc. **37**, 18 (1954).
87. R.M. Pilliar and J. Nutting, Philos. Mag. **6**, 181 (1967).
88. R.T.K. Baker, J.J. Chludzinski, C.A. Bernardo, and J.L. Figueiredo, in "Proceedings 9th International Congress on Catalysis, Calgary, 1988", edited by M.J. Phillips and M. Ternan (Chem Institute of Canada, Ottawa, 1988), Vol. 3, p. 1059.
89. R.T.K. Baker, J.J. Chludzinski, Jr., and R.D. Sherwood, Carbon **23**, 245 (1985).
90. J. Guinot, M. Audier, M. Coulon, and L. Bonnetain, Carbon **19**, 95 (1981).
91. G.A. Jablonski, F.W.A.H. Geurts, and A. Sacco, Jr., Carbon **30**, 99 (1992).
92. R. Lamber, N. Jaeger, and G. Schulz-Ekloff, Surf. Sci. **197**, 402 (1988).
93. M. Arai, T. Ishikawa, T. Nakayama, and Y. Nishiyama, J. Colloid and Interface Sci. **97**, 254 (1984).
94. M. Audier, M. Coulon, and L. Bonnetain, Carbon **17**, 391 (1979).
95. R.T.K. Baker and R.J. Waite, J. Catal. **37**, 101 (1975).
96. N.M. Rodriguez, M.S. Kim, and R.T.K. Baker, J. Catal. (in press).
97. J. Maire and J. Mering, in *Chemistry and Physics of Carbon* (Marcel Dekker, New York, 1970), Vol. 6, p. 125.
98. W.T. Owens, N.M. Rodriguez, and R.T.K. Baker, Preprints, Div. of Petrol. Chem., ACS (in press).
99. H. Jaeger, V.W. Maslen, and McL. Mathieson, Carbon **30**, 269 (1992).
100. S.J. Gregg and K.S.W. Sing, *Adsorption, Surface Area and Porosity,* 2nd ed. (Academic Press, London, 1982).
101. N.M. Rodriguez, M.S. Kim, W.B. Downs, and R.T.K. Baker, in *Carbon Fibers, Filaments and Composites,* edited by J.L. Figueiredo, C.A. Bernardo, R.T.K. Baker, and K.J. Huttinger,

NATO ASI Series (Kluwer Academic Publishers, Dordrecht, The Netherlands, 1987), Vol. 177, p. 541.
102. N. M. Rodriguez, unpublished results.
103. T. Meguro, N. Torikai, N. Watanabe, and I. Tomizuka, Carbon **23**, 137 (1985).
104. N. M. Rodriguez, T. Yokono, N. Takahashi, Y. Sanada, and H. Marsh, Fuel **66**, 1743 (1987).
105. R. T. K. Baker, G. R. Gadsby, R. B. Thomas, and R. J. Waite, Carbon **13**, 211 (1975).
106. W. B. Downs and R. T. K. Baker, Extended Abstracts, 20th Biennial Conference on Carbon, Santa Barbara, CA (1991), p. 318.
107. A. Espinola, P. Mourente Miguel, M. Roedel Salles, and A. Ribeiro Pinto, Carbon **24**, 337 (1986).
108. D. M. Smith, W. F. Welch, S. M. Graham, A. R. Chughtai, B. G. Wicke, and K. A. Grady, Appl. Spec. **42**, 674 (1956).
109. E. D. Ermenc, Chem. Eng. Prog. 448 (1956).
110. W. Jorthe, A. T. Bell, and S. Lynn, Ind. Eng. Chem. Process Des. Dev. **11**, 434 (1972).
111. K. Kaneko, Langmuir **3**, 357 (1987).
112. K. Kaneko, Colloid Surf. **37**, 115 (1989).
113. J. W. Geus, private communication.
114. D. W. McKee and V. J. Mimeault, in *Chemistry and Physics of Carbon* (Marcel Dekker, New York, 1973), Vol. 8, p. 151.
115. J. Delmonte, *Technology of Carbon and Graphite Fiber Composites* (Van Nostrand Reinhold Co., New York, 1981).
116. P. Ehrburger, in *Carbon Fibers, Filaments and Composites,* edited by J. L. Figueiredo, C. A. Bernardo, R. T. K. Baker, and K. J. Huttinger, NATO ASI Series (Kluwer Academic Publishers, Dordrecht, The Netherlands, 1989), Vol. 177, pp. 147–161.
117. E. Fitzer, K. H. Geigl, W. Huttner, and R. Weiss, Carbon **18**, 389 (1980).
118. L. T. Drzal, M. J. Rich, and P. F. Lloyd, J. Adhesion **16**, 1 (1982).
119. I. K. Ismail and M. D. Vangness, Carbon **26**, 749 (1988).
120. P. Pattabiraman, N. M. Rodriguez, B. Z. Jang, and R. T. K. Baker, Carbon **28**, 867 (1990).
121. E. Fitzer, *Carbon Fibres and their Composites* (Springer-Verlag, Berlin, 1985).
122. K. K. Chawla, *Composite Materials* (Springer-Verlag, New York, 1987).
123. E. de Lamotte and A. J. Perry, Fibre Sci. Technol. **3**, 157 (1970).
124. F. A. Posey and J. Morozumi, J. Electrochem. Soc. **113**, 176 (1966).
125. W. Tiedemann and J. Newmann, J. Electrochem. Soc. **122**, 70 (1975).
126. M. Matsumoto, T. Hashimoto, Y. Uchiyama, and K. Murata, Carbon (in press).